Journal of Structural Geology, Vol. 5, No. 6, pp. 497 to 506, 1983
Printed in Great Britain

0191-8141/83 $3.00+0.00
Pergamon Press Ltd.

Displacement and strain patterns from naturally occurring shear zone terminations

CAROL SIMPSON

Department of Geology, Oklahoma State University, Stillwater, OK 74078, U.S.A.

(*Received* 28 *February* 1983; *accepted in revised form* 1 *June* 1983)

Abstract—Strain distribution patterns are described from several naturally occurring ductile shear zone terminations and a two-fold classification is suggested. Type I termination patterns show a symmetrical decrease in strain area and intensity, and are associated with very low shear strain (γ) values in the main shear zone. The more common Type II termination patterns show a symmetrical increase in strain area with decrease in strain intensity. Some brittle–ductile examples of Type II terminations contain secondary shears that resemble splay faults. All the available evidence suggests that the deformation near the terminations of these shear zones is not plane strain, nor do the observed strain patterns readily fit the existing theoretical models.

INTRODUCTION

THE DISTRIBUTION of finite strain and displacement at the termination of ductile and brittle–ductile shear zones is generally complex (Freund 1974, Ramsay 1980). From a large range of possible models, Ramsay & Allison (1979) and Ramsay (1980) have suggested two end-members to be the most geologically reasonable. In the plane strain model, boundary deflections are constrained and the tips of dextral shear zones show a tendency to bend in a clockwise sense, and sinistral shear zones tend to bend in an anticlockwise sense. In the non-plane strain model, extension and shortening deformation patterns are set up on either side of the shear zone tip and all displacements occur in the Y direction of finite strain, normal to the shear zone profile. The second of these two models is similar to that proposed by Coward (1976) to explain pure-shear deformation patterns at the leading edges of developing ductile shear zones. In both cases, for the deformation in the central part of the main shear zone to be plane strain simple shear, the displacements at the shear zone tips must gradually die out over a progressively wider area into undeformed rock (Ramsay & Allison 1979).

However, there are few descriptions of finite strain distributions in naturally occurring ductile shear zone termination regions with which to test these kinematic models (Freund 1974, Ramsay & Allison 1979). On the other hand, brittle strike–slip fault terminations have received considerable attention in the literature (e.g. Anderson 1951, Chinnery 1966, Freund 1974, Segall & Pollard 1983). This paper presents observations of strain and displacement in and around several narrow (cm-scale width) shear zones that terminate within relatively undeformed igneous rock. Ductile terminations of shear zones and incipient shear zones are described from the core of the Maggia Nappe in the Lepontine Alps, and brittle–ductile terminations are illustrated from the Roses (Rosas) granodiorite, NE Spain. In each area the outcrops comprise reasonably planar polished surfaces that are approximately parallel to the shear zone profile sections.

DUCTILE SHEAR ZONES IN MAGGIA GNEISS

Geological setting

Almost completely undeformed late-Hercynian granites and adamellites form one of the main lithological units of the core of the Maggia Nappe, a Lower Pennine basement nappe in the Lepontine Alps (Preiswerk 1918, Günthert 1954, Ramsay & Allison 1979, Simpson 1981, 1982). At the margins of cm to tens of metre width, amphibolite grade, ductile shear zones of Alpine age, a new shear-zone related foliation has been observed (Ramsay & Graham 1970, Ramsay & Allison 1979). The aspect ratios of quartz, biotite and feldspar grain aggregates gradually change with increasing strain from equidimensional, or very slightly ellipsoidal, in the undeformed rock to platy within the shear zones (Simpson 1983). All minerals were deformed in a ductile manner by dynamic recrystallization processes. No evidence for any significant volume change was found in any of these shear zones, the deformation being essentially isochemical (Kerrich *et al.* 1977, Simpson 1981). Several cm-scale shear zones and incipient shear zones occur in remnant lozenge-shaped pods of relatively undeformed granitic rock within a network of anastomosing metre-scale shear zones (Simpson 1981, 1983). In almost every example studied, each of the small-scale shear zones within any one remnant pod has the same sense of displacement as the surrounding major ductile shear zones. Many of the small shear zones can be traced from major shear zones into undeformed rock where they terminate.

Incipient ductile shear zones in Maggia gneiss

In the Maggia granitic gneiss roughly equidimensional biotite and quartz grain aggregates within the unsheared rock are deformed to ellipses (on the two-dimensional outcrop surface) within incipient narrow, planar-sided shear zones (Fig. 1). These zones are generally only 10 or 20 cm long by one or two cm wide (i.e. one or two grain aggregates in width) and within them the long axes of the elliptical aggregates are oriented at approximately 43° to

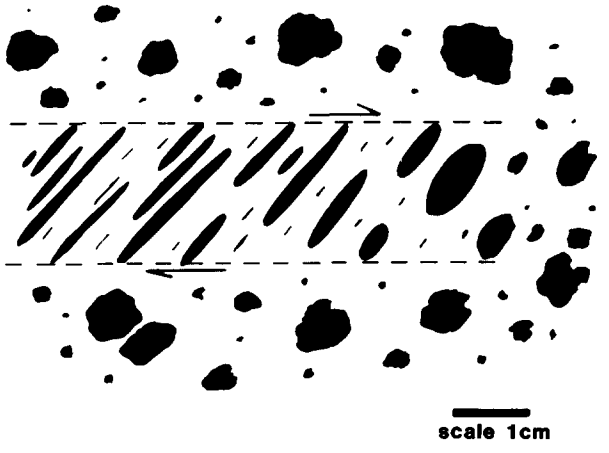

Fig. 1. Schematic representation (profile view) of the right-hand tip of an incipient right-lateral ductile shear zone in Maggia granitic gneiss, drawn from field sketches. Biotite grain aggregates shown in black, quartz and feldspar aggregates not illustrated. Dashed lines represent the incipient shear zone boundaries within which grain aggregates have an elliptical shape.

the zone boundaries. Assuming that these deformed grain aggregates lie close to the *XY* plane of the finite strain ellipsoid (Ramsay & Graham 1970), then the sense and amount of movement across these incipient shear zones is readily determined. In each example observed, the sense of shear was the same as that of nearby fully developed ductile shear zones, and the strain was not greater than $\gamma = 0.35$.

A careful examination of the terminations of the incipient shear zones revealed no discernable deflection of the zone orientation, nor any widening of the region of strain. No evidence for any change in orientation of the long axes of elliptically shaped mineral aggregates could be detected as a function of position along the zones. The only difference between the incipient shear zone centres and terminations is a decrease in ellipticity of the grain aggregates at the tips of the zones as the visible shear strain decreases to zero (Fig. 1).

Ductile shear zone terminations

Figure 2 illustrates the termination of a small ductile shear zone in an outcrop of adamellite where the wall rocks contain a very weak but relatively homogeneous planar fabric. This fabric is defined by a preferred shape orientation of ellipsoidal biotite and quartz grain aggregates at about 45° to the shear zone boundary, and by a parallel alignment of the long dimensions of scattered 2–3 mm muscovite flakes. With increasing shear strain the grain aggregates within the shear zone assume a more platy aspect (Simpson 1983) and so define a new foliation that is aligned at progressively smaller angles to the shear zone boundary (Ramsay & Graham 1970). At the termination of this shear zone, the foliation gradually changes in orientation to become parallel to, and indistinguishable from, the weak planar fabric in the wall rocks (Fig. 2). As this change in orientation of foliation occurs, the zone of discernible shear strain widens symmetrically with respect to the strike of the zone. No significant deflection in orientation of the shear zone ends were observed.

In shear zones with deformed walls, as in Fig. 2, the components of strain are (i) homogeneous strain, (ii) simple shear and (iii) a volume change $(1 + \Delta)$ perpendicular to the boundaries of the zone (Ramsay 1980). Separation of the simple shear and volume change components is theoretically possible provided that the wall rocks contain strain markers and that a marker line (e.g. a vein or dyke) is deflected through the zone. The shear zone illustrated in Fig. 2 does not contain any deflected marker lines. However, the ellipticity of the strain ellipse in the wall rocks can be approximately estimated at $R = 4$, assuming that the small amphibolite xenolith was originally equidimensional. If the volume change $(1 + \Delta)$ is assumed to be zero, then it is possible to estimate the shear strain (γ) as a function of distance across the shear zone (Fig. 2). These profiles are constructed at various positions along the strike of the zone. The numerical values for shear strain given in Fig. 2 are uncertain due to the ignored volume changes and the possibility of non-equidimensional undeformed xenoliths. However, if the volume changes are small or at least uniform along the strike of the zone, the general patterns shown are probably reasonable reflections of the variation in shear strain. Thus, the shear zone termination in Fig. 2 shows a symmetrical increase in width of the zone as the shear strain component parallel to the zone systematically decreases in magnitude.

In Fig. 3 a small ductile shear zone terminates within a part of a remnant pod of granite that otherwise records no visible finite strain. A very thin aplite dyke is displaced by this zone near its end. As in the previously described example, the shear strain is symmetrically spread over an increasingly wide area as the orientation of the foliation trace gradually changes to lie uniformly at about 43° to the shear zone walls (Fig. 3). The symmetric increase in width of the zone is illustrated by comparing the width of the shear zone (at the extreme left-hand side of Fig. 3) to the length of the deformed aplite dyke in the more diffuse area of lower strain near the end of the zone (right-hand side of Fig. 3). A few cm to the right of the deflected aplite dyke, the last detectablefabric in the zone is subparallel to the foliation at the shear zone boundary, that is at about 45° to the margins of the shear zone.

Shear strains (γ) as a function of position across the shear zone are shown for a number of positions along the length of the zone (Fig. 3). The shear strain (γ) is found from the angular relationship (θ') between the foliation and the shear zone boundary (Ramsay & Graham 1970, Ramsay 1980), where

$$\gamma = \frac{2}{\tan 2\theta'}. \qquad (1)$$

The shear strain profiles become flatter near the end of the zone as the zone widens and the foliation becomes progressively weaker and more difficult to discern. Although the intensity of shear strain is asymmetrically distributed across the shear zone, the widening of the shear zone is symmetric.

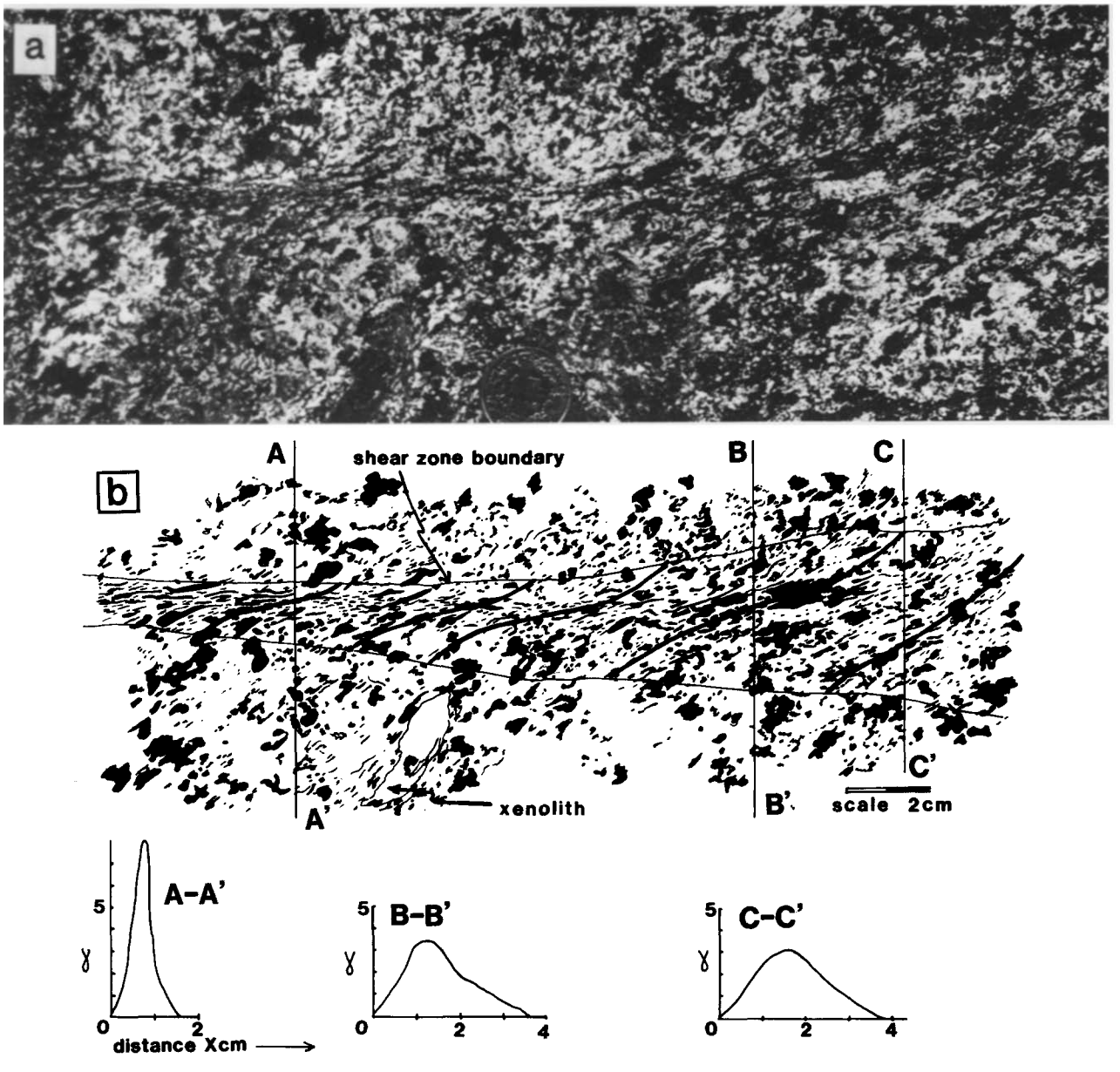

Fig. 2. Termination of a right-lateral ductile shear zone in Maggia granitic gneiss that contains a weak planar fabric. (a) Photograph of outcrop, coin diameter is 2.4 cm. (b) Tracing from photograph to illustrate change in schistosity trace orientation and widening of strained area towards termination. Schistosity defined by biotite aggregates (black) and quartz/feldspar grain aggregates (not illustrated). Shear zone boundary taken as first deviation of schistosity trace from orientation of fabric in wall rocks. Note parallelism between orientation of wall rock fabric and that of last visible shear zone fabric in termination region. Shear strain (γ)/distance profiles along lines A–A′, B–B′ and C–C′ are drawn assuming zero volume change.

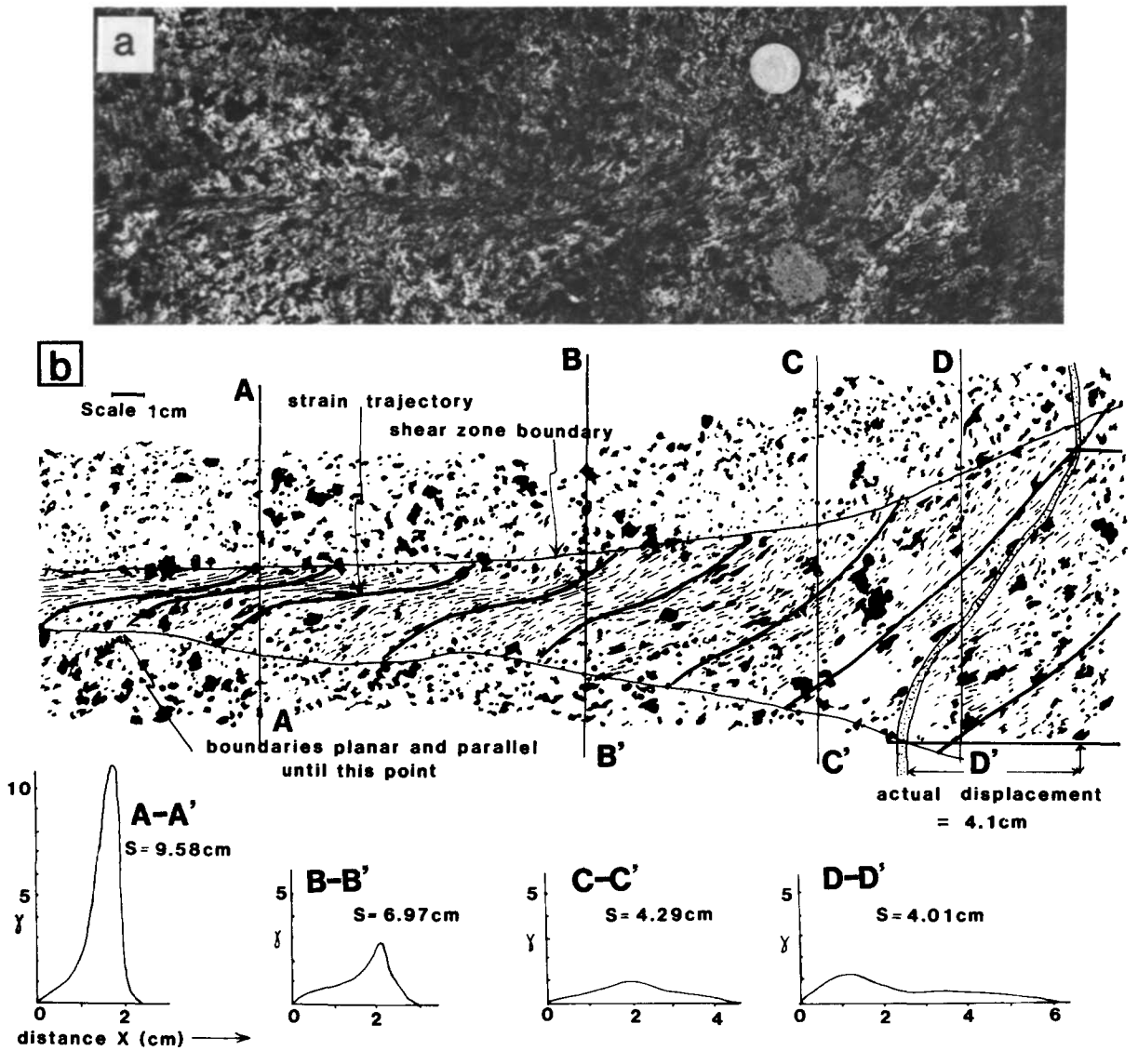

Fig. 3. Termination of a small right-lateral ductile shear zone in unfoliated Maggia granitic gneiss. (a) Photograph of outcrop, coin diameter is 2.4 cm. (b) Tracing from photograph to illustrate change in schistosity trace orientation and widening of zone of shear strain towards termination. Schistosity defined by elongate biotite aggregates (black) and quartz/feldspar grain aggregates (not illustrated). Heavy lines represent schistosity trace. Small aplite dyke is marked in stipple on right hand side of shear zone, in the termination region. Corresponding γ/distance profiles and displacements (S) estimates are drawn at intervals A–A′, B–B′, C–C′ and D–D′ along the zone.

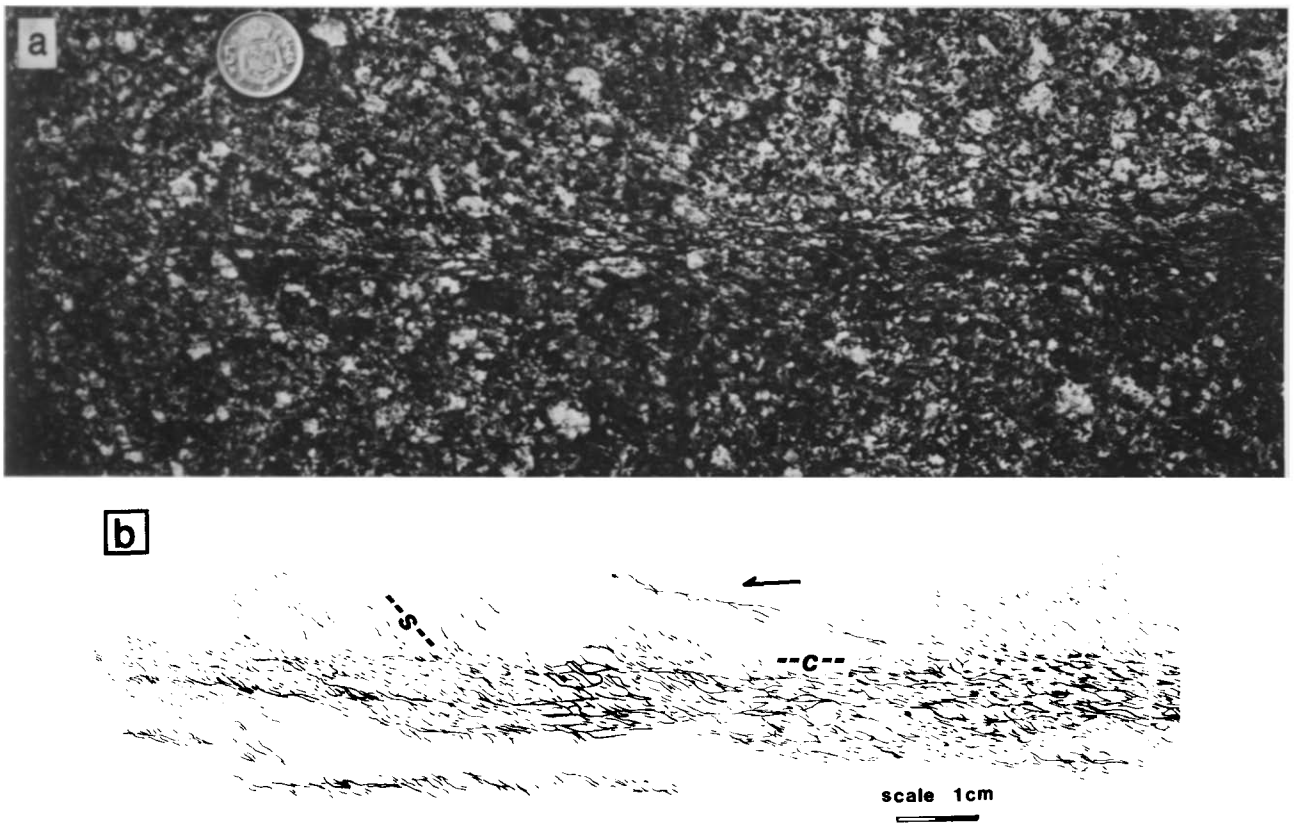

Fig. 5. Termination of a narrow left-lateral shear zone in Roses granodiorite. (a) Photograph of outcrop, coin diameter is 2.4 cm. (b) Tracing from photograph to illustrate the 's' and 'c' surfaces (see text for discussion). There is no obvious spreading of the shear strain or curvature of the shear zone tip.

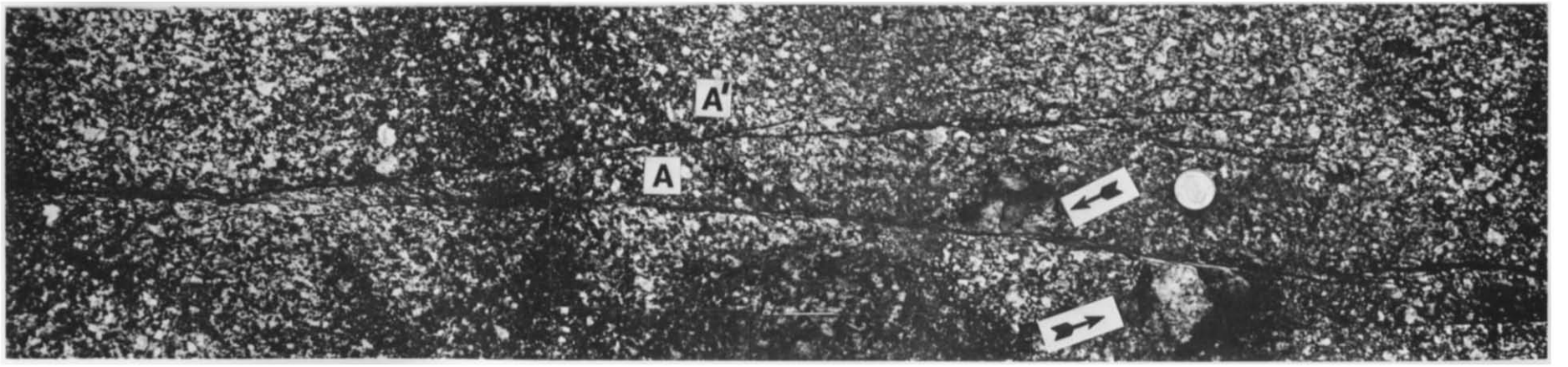

Fig. 8. Narrow left-lateral ductile shear zone (lower) with brittle secondary shears (upper) in Roses granodiorite. The small composite xenolith (arrowed) can be traced continuously across the ductile shear zone. The secondary shear zone offsets the mafic schlieren (A–A'), also with a left-lateral movement sense, and becomes narrower and more brittle towards its termination.

The total displacement across the zone can be estimated from

$$S = \int_0^x \gamma \, dx \qquad (2)$$

(Ramsay & Graham 1970, Ramsay 1980). The displacement (S) shows a decrease with decrease in maximum shear strain toward the termination of the zone (Fig. 3), suggesting a departure from plane strain conditions towards the tip of the shear zone (Ramsay & Allison 1979). The measured offset of the aplite dyke was 4.1 cm whereas using equation (2) above gave a displacement estimate of 4.0 cm in this termination region of the shear zone. This close agreement is the more remarkable when it is considered that implicit in the estimation method is the assumption of planar, parallel sided shear zone boundaries (Ramsay & Graham 1970), an assumption that is not well satisfied in the termination region of this shear zone.

BRITTLE–DUCTILE SHEAR ZONE TERMINATIONS IN ROSES GRANODIORITE

Situated approximately 120 km northeast of Barcelona, Spain, the Roses granodiorite is the easternmost late-Hercynian intrusive body in the Axial Zone of the Pyrenees. Both the granodiorite and its metasedimentary host rocks of presumed Upper Ordovician age have been affected by post-intrusive deformation (Carreras 1973, Carreras & Losantos 1982, Simpson *et al.* 1982). This deformation is thought to be of very late Hercynian age and takes the form of ductile and brittle–ductile shear zones in the granodiorite with minor crenulation folds in the metasediments (Carreras & Losantos 1982, Simpson *et al.* 1982).

The sequence of deformation events in the granodiorite began with the formation of a weak linear and planar fabric by dynamic recrystallization of constituent minerals under upper-greenschist facies conditions (Simpson *et al.* 1982). This event was followed by the formation of an anastomosing network of ductile shear zones, cm to tens of metres in width, under lower-greenschist facies conditions. Under these latter conditions the feldspar in the rock deformed by microfracturing whereas quartz and some biotite grains deformed in a ductile manner by dynamic recrystallization. Most mafic minerals within the shear zones are altered to chlorite and epidote, and a new growth of muscovite and albite grains is commonly observed (Simpson *et al.* 1982). The latest shear zones to form are much narrower than the earlier-formed ductile shear zones and are often seen to terminate within more or less undeformed lenses or pods of granodiorite (Fig. 4, squares B1 and C1). Figure 5 illustrates one such termination in greater detail: no obvious spread of the shear strain at the shear zone tip can be detected. In thin-section and in outcrop two distinct orientations of fabric can be discerned in the shear zone. These correspond to (i) foliation or 's' surfaces that are inclined at 30–40° to the shear zone boundaries, and (ii) discrete slip or 'c' surfaces that are roughly parallel to the shear zone boundaries (Berthé *et al.* 1979, Simpson & Schmid in press). Both surfaces are defined by fine-grained chlorite, muscovite, epidote and biotite surrounding fractured feldspars and dynamically recrystallized quartz grains. Offset along the zone has occurred primarily on the 'c' surfaces of relatively high strain: the dominant orientation of the 's' surfaces at about 30° to the shear

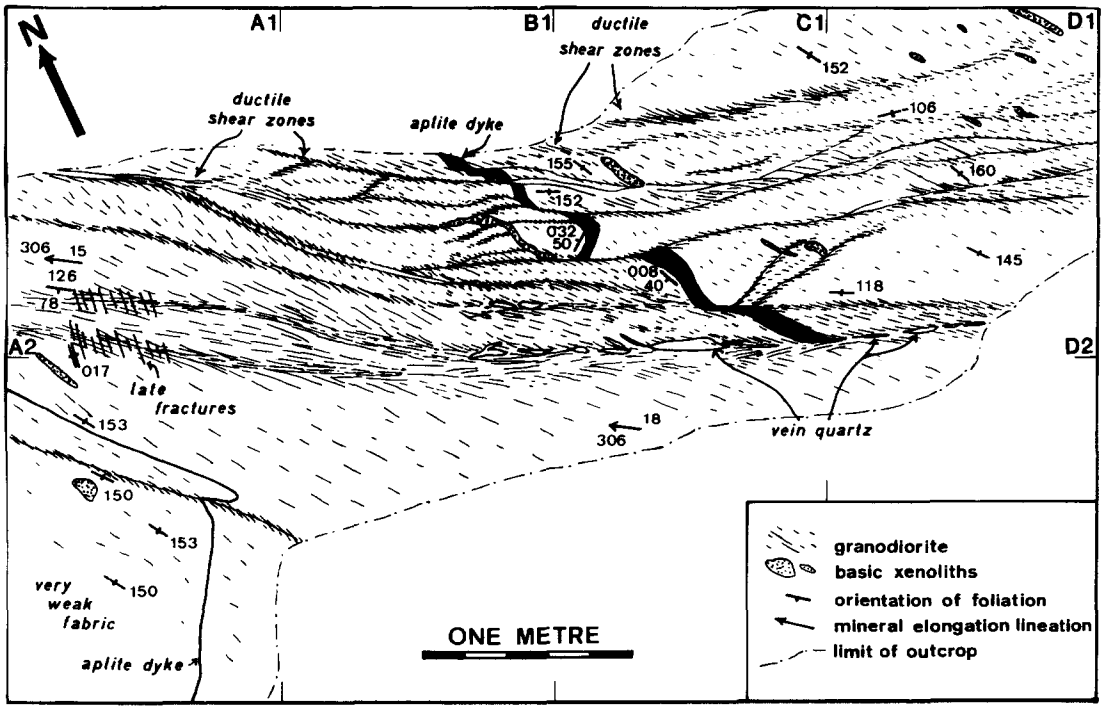

Fig. 4. Map of a small section of a left-lateral shear zone in granodiorite from Roses, NE Spain. The shear zone comprises an anastomosing network of narrow left-lateral ductile shear zones that offset the small aplite dyke and surround the lozenge-shaped areas of lower finite strain.

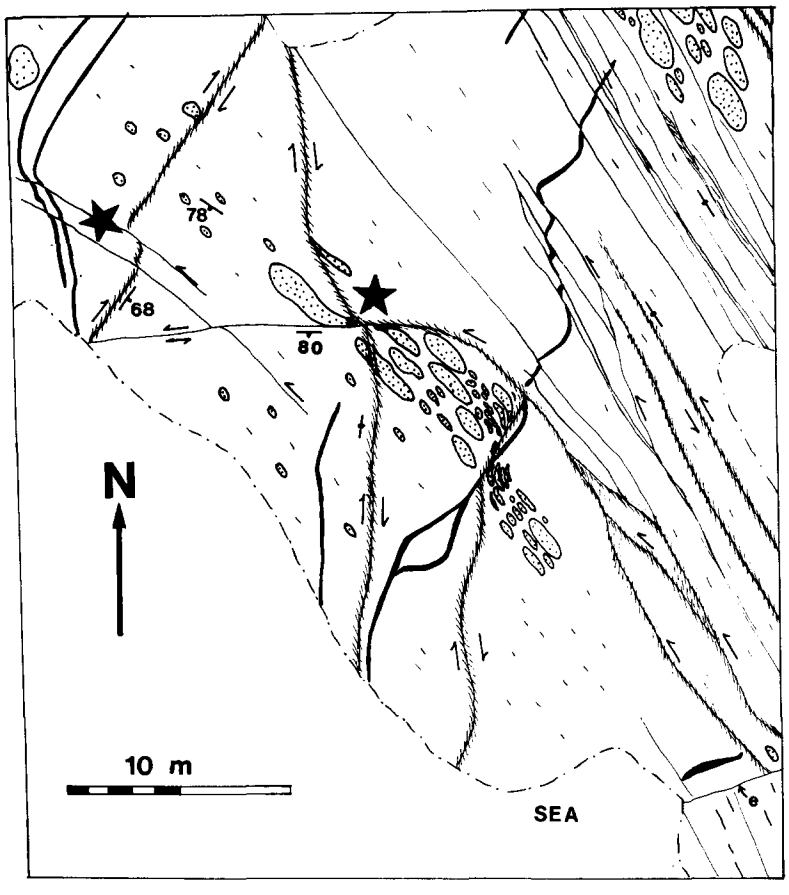

Fig. 6. Map of brittle–ductile shear zones in Roses granodiorite. Continuous heavy lines are thin aplite dykes, otherwise legend as for Fig. 4. Narrow shear zones become brittle shear fractures at their tips. Brittle shears also offset earlier ductile shear zones (marked by stars) as well as aplite dykes.

zone boundaries indicates that between 'c' surfaces, γ rarely exceeds 1.0. As the visible strain in the rock diminishes to zero, the 'c' planes occur with less frequency until the last visible fabric in the rock is that of the 's' planes oriented at about 40° to the main shear zone boundary (Fig. 5).

Many left-lateral shear zones in the Roses granodiorite are less than one cm wide and show a very poorly developed foliation that vanishes completely towards the termination of the shear zones so that the tips are essentially brittle fractures. These brittle shears offset earlier ductile shear zones as well as the aplite dyke (Fig. 6, areas of interest marked by stars). In some instances a single ductile shear zone terminates in a single brittle fracture but more commonly a shear zone divides into several narrow zones that become brittle fractures as the visible strain in the rock dies away to zero. Figure 7 illustrates a single termination zone in more detail. The main 5-cm wide, left-lateral shear zone divides into several narrower left-lateral zones. These narrower shear zones subdivide in turn into brittle shear fractures that terminate a short distance into the undeformed rock. A weak foliation is often visible in the rock between shear fractures but seldom along the immediate walls of the fractures. The overall geometry of this termination zone is similar to that of the type A mode of secondary faulting described by Chinnery (1966). Some of the main narrow ductile shear zones have secondary shear zones branching from them; these have the geometry of McKinstry's (1953) second-order shears and the type C fractures of Chinnery (1966). The example illustrated in Fig. 8 shows a small aplite/amphibolite xenolith which can be traced continuously across 11.5 cm of left-lateral displacement on the lower ductile shear zone. Shear strain on this zone is approximately $\gamma = 22$. The secondary shear zone branching from the lower ductile zone also has a left-lateral movement sense as illustrated by the displaced biotite-rich schlieren (A–A′ on Fig. 8) and by the very localized development of a foliation along the edge of the shear fracture. Elsewhere the secondary shear surface is entirely brittle in nature and has tertiary shears (seen as hairline shear joints) branching from it. At its termination the secondary shear divides into a series of fine cracks across which no discernible displacement has occurred. These cracks then terminate in completely undeformed granodiorite. The geometry of this termination zone is similar to that of Chinnery's (1966) type A secondary fault system.

DISCUSSION

The small ductile and brittle–ductile shear zone terminations described from the Maggia and Roses rocks show two distinctive patterns of strain distribution. Type I terminations, both ductile and brittle–ductile, are those

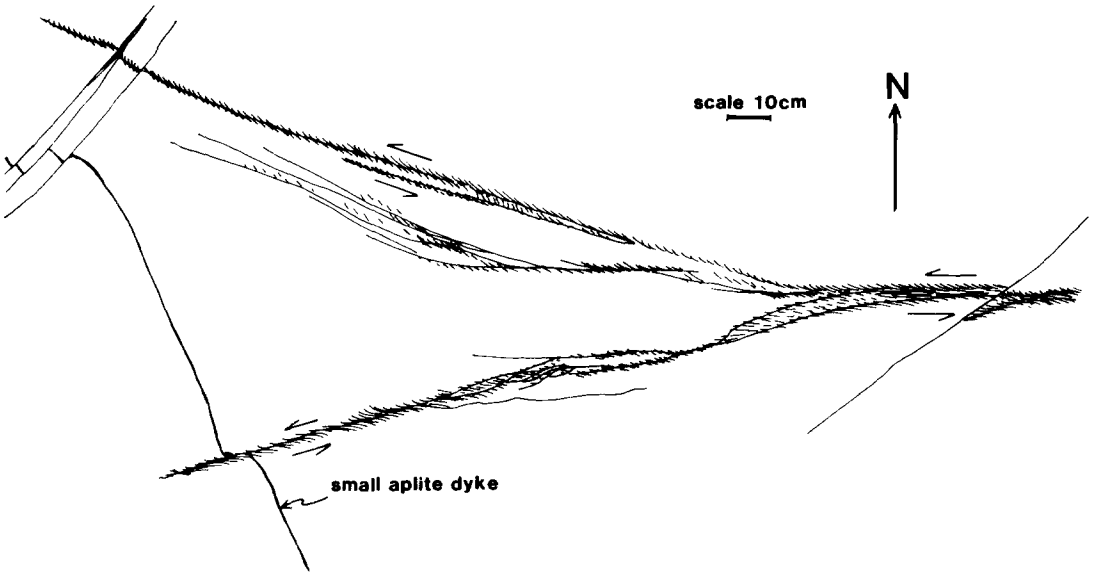

Fig. 7. Map illustrating the termination of a brittle–ductile shear zone in Roses granodiorite. The shear zone divides into several splay shears that terminate after a short distance into joints and then undeformed rock.

in which a simple decrease in shear strain occurs along the zone without the zone width increasing, or the zone trace curving significantly in the profile section (Figs. 1 and 5). This strain pattern has only been observed in incipient shear zones and those with very low shear strains. Because the displacements at the Type I terminations do not die out over a progressively wider area in the profile section, the deformation in these very low strain zones is probably not that of plane strain simple shear but is more likely a combination of simple shear and heterogeneous pure shear.

The more common Type II terminations, both ductile and brittle–ductile, show a pattern of a visible symmetrical spreading of the shear strain region in the profile section as the shear strain and displacement fall to zero (Figs. 2, 3 and 7). No evidence has been found for significant curvature of the tips as the visible shear strain decreases, even though the main portion of the shear zones themselves are often slightly curvi-planar.

Thus, neither the Type I nor the Type II terminations appear to fit either of the two end-member models of Ramsay & Allison (1979) and Ramsay (1980). The deformation in these terminations was almost certainly not that of plane strain but no evidence was found for the predicted compressional and extensional strain patterns at the shear zone tips. Unfortunately, the nature of the outcrops in both study areas precluded the examination of these zones in the third dimensions (i.e. the Y direction of finite strain), and so the strong possibility remains that much of the strain was taken up by displacements in the Y direction.

As illustrated in Figs. 7 and 8, the Roses Type II brittle–ductile terminations show a number of features in common with secondary faults associated with strike–slip faulting. Several authors have addressed the problem of stress conditions governing the initiation and orientation of secondary, or splay, faults at the terminations of strike–slip faults (e.g. Anderson 1951, McKinstry 1953, Moody & Hill 1956, Chinnery 1963, 1966). It has been suggested that secondary faulting is less likely to occur where the displacement decays gradually along the length of the fault: therefore, the presence of the splays may indicate a rapid decay to zero of the displacement at the tip of the main fault (Chinnery 1963, 1966). The Roses shear zone terminations only show splay-like features (i.e. Type II terminations) where the shear strain in the main zone is reasonably high: no splays have been observed at the ends of shear zones with very low strain (Type I terminations). These observations lend support to Chinnery's (1966) model for high displacement gradients at the Type II terminations. However, Freund (1974) has shown that a displacement decay is not necessary and that the total horizontal displacements may remain more or less constant but be divided among the splay faults, provided that ductile deformation between the splays can counteract any tendency to produce gaps or overlaps. It was not possible to determine accurately the displacement along every splay of the Roses Type II terminations, but wherever this was attempted the displacement clearly reduced to zero over a short distance at the tips of the splays, an observation which again supports the Chinnery (1966) model.

One outstanding problem pertaining to the Roses Type II terminations is that of the relative timing of the ductile and brittle modes of failure. Segall & Pollard (1983) have successfully demonstrated that ductile deformation within small-scale strike–slip faults in granite of the Sierra Nevada batholith was preceded by brittle failure of the rock along extension joints. The zero apparent displacement at the tips of the splays in the Roses Type II terminations, may indicate that these, too, initiated as extension and not as shear fractures. However, it is also quite possible that initial ductile deformation of the Roses granodiorite was followed by progressively more brittle behaviour. Indeed, there is

ample independent evidence from elsewhere in the Roses region to support a ductile to brittle progression (Simpson *et al.* 1982). A programme of work to investigate the relative timing of the failure modes is presently underway.

CONCLUSIONS

Strain distribution patterns associated with naturally occurring ductile and brittle–ductile shear zone terminations in the Maggia and Roses granitoids fall into two main categories: Type I patterns, which show a symmetrical decrease in the area of finite strain and in strain intensity, and Type II patterns, which show a symmetrical increase in the strained area as strain intensity decreases.

None of the Type I or Type II terminations described appear to fit either of the models presented by Coward (1976), Ramsay & Allison (1979) and Ramsay (1980). Type I patterns are associated with very low strain shear zones where the deformation was probably not that of plane strain simple shear. Type II strain patterns are associated with those shear zones that exhibit simple shear deformation along the main part of the zone but show a departure from plane strain conditions at the tips. In all probability most of the strain at the Type II tips was taken up in the Y direction of finite strain.

The rapid decay of displacement along the splay-like features in some of the more brittle Type II terminations may indicate that displacements along the main shear zone also underwent a rapid decay to zero at this point (Chinnery 1966). However, whether brittle or ductile failure was the first to occur in these brittle–ductile zones remains unresolved at present.

Finally, it must be stressed that the simple, two-fold classification presented here is not meant to be complete. Gradations undoubtedly occur between symmetrical strain distribution patterns at shear zone terminations and asymmetrical ones, such as those described by Ramsay & Allison (1979).

Acknowledgements—This work was funded in part by the Zentenarfonds of the ETH, Zürich, Switzerland, and in part by National Science Foundation Grant EAR 8121438. Helpful discussions at various stages of the work with J. G. Ramsay, M. Casey, S. M. Schmid and P. Segall, are acknowledged with thanks, although the author takes full responsibility for the interpretations put forward here. Thanks are also due to J. Carreras for introducing the author to the Roses area and for providing logistical support during field work in Spain. The manuscript was much improved thanks to critical reviews by P. Segall and two anonymous referees. R. N. Donovan read an earlier draft of the manuscript, and P. Ashcraft and J. Donovan provided invaluable secretarial assistance.

REFERENCES

Anderson, E. M. 1951. *The Dynamics of Faulting*. (2nd ed.) Oliver & Boyd, Edinburgh.

Berthé, D., Choukroune, P. & Jegouzo, P. 1979. Orthogneiss, mylonite and non-coaxial deformation of granites: the example of the South Armorican shear zone. *J. Struct. Geol.* **1**, 31–42.

Carreras, J. 1973. Petrologia y analisis estructural de las rocas metamorficas en la zone del Cabo de Creus (Prov. de Gerona). Unpublished Ph.D. thesis, University of Barcelona, Spain.

Carreras, J. & Losantos, M. 1982. Geological setting of the Roses Granodiorite (E. Pyrenees, Spain). *Acta geol. Hispánica* **4**, 211–218.

Chinnery, M. A. 1963. The stress changes that accompany strike-slip faulting. *Bull. seism. Soc. Am.* **53**, 921–932.

Chinnery, M. A. 1966. Secondary faulting. I. Theoretical aspects, II. Geological aspects. *Can. J. Earth Sci.* **3**, 163–190.

Coward, M. P. 1976. Strain within ductile shear zones. *Tectonophysics* **34**, 181–197.

Freund, R. 1974. Kinematics of transform and transcurrent faults. *Tectonophysics* **21**, 93–134.

Günthert, A. 1954. Beitrage zur Petrographie und Geologie des Maggia-Lappens (N.W. Tessin). *Schweiz. miner. petrogr. Mitt.* **34**, 1–159.

Kerrich, R., Fyfe, W. S., Gorman, B. E. & Allison, I. 1977. Local modification of rock chemistry by deformation. *Contr. Miner. Petrol.* **65**, 183–190.

McKinstry, H. E. 1953. Shears of the second order. *Am. J. Sci.* **251**, 401–414.

Moody, J. D. & Hill, M. J. 1956. Wrench fault tectonics. *Bull. geol. Soc. Am.* **67**, 1207–1246.

Preiswork, H. 1918. *Geologische Beschreibung der Lepontinischen Alpen*. Beitrage zur Geologische Karte der Schweiz, 26.

Ramsay, J. G. 1980. Shear zone geometry: a review. *J. Struct. Geol.* **2**, 83–99.

Ramsay, J. G. & Allison, I. 1979. Structural analysis of shear zones in an Alpinised Hercynian Granite. *Schweiz. miner. petrogr. Mitt.* **59**, 251–279.

Ramsay, J. G. & Graham, R. H. 1970. Strain variations in shear belts. *Can. J. Earth Sci.* **7**, 786–813.

Segall, P. & Pollard, D. D. 1983. Nucleation and growth of strike-slip faults in granite. *J. geophys. Res.* **88**, 555–568.

Simpson, C. 1981. Ductile shear zones: a mechanism of rock deformation in the orthogneisses of the Maggia Nappe, Ticino, Switzerland. Unpublished Ph.D. thesis, ETH Zürich, Switzerland.

Simpson, C. 1982. The structure of the northern lobe of the Maggia Nappe, Ticino, Switzerland. *Eclog. geol. Helv.* **75**, 495–516.

Simpson, C. 1983. Strain and shape fabric variations associated with ductile shear zones. *J. Struct. Geol.* **5**, 61–72.

Simpson, C. & Schmid, S. M. in press. An evaluation of criteria to deduce the sense of movement in sheared rocks. *Bull. geol. Soc. Am.*

Simpson, C., Carreras, J. & Losantos, M. 1982. Inhomogeneous deformation in Roses granodiorite, N.E. Spain. *Acta geol. Hispánica* **4**, 219–226.